

Understanding and Controlling Turbulent Mixing in a Laboratory Magnetosphere

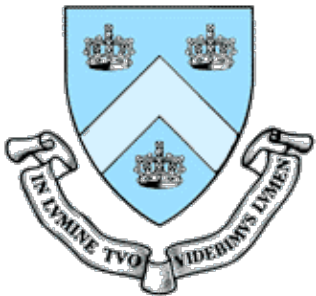
Mike Mael

Department of Applied Physics and Applied Math, Columbia University, New York, NY USA

*(Acknowledging the work from many former students and collaborators including
Darren Garnier, Jay Kesner, Max Roberts, Ben Levitt, Brian Grierson)*

58th Annual Meeting of the APS Division of Plasma Physics
San Jose, CA

Poster Session TP10 (Session VII) – November 3, 2016

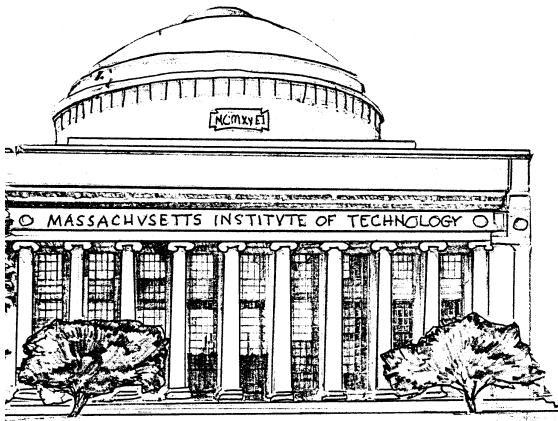


With Sincere Apologies...

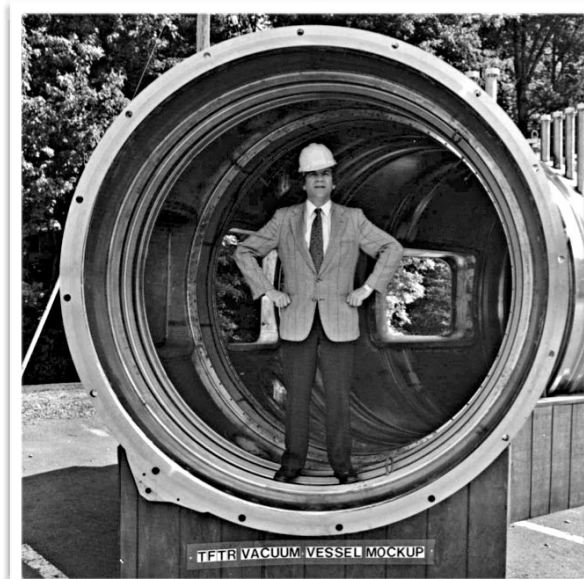
Mike Mauel is chair of Invited Session TI3 (*now*):

Non-neutral Plasmas, Fusion, and Beams: The Legacy of Ron Davidson

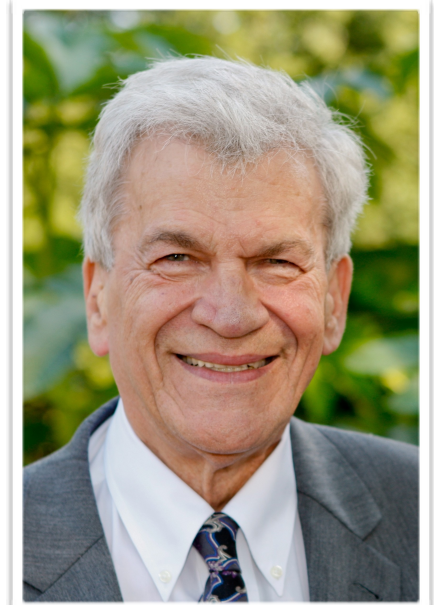
FUSION
POWER
AT
MIT



Professor of Physics
Director, PFC
(1978-1991)



Director, PPPL
(1991-1996)



Editor-in-Chief
(1991-2015)

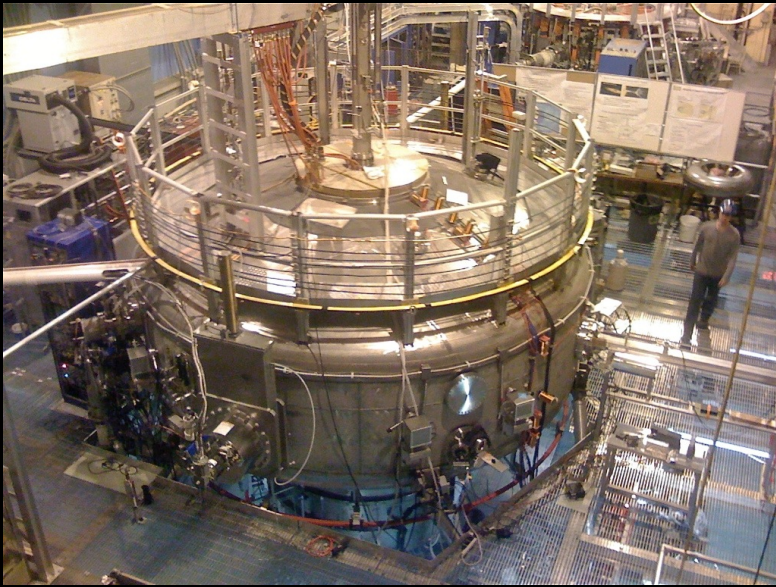
Abstract

In a laboratory magnetosphere, plasma is confined by a strong dipole magnet, and complex nonlinear processes can be studied and controlled in near steady-state conditions. Because a dipole's magnetic field resembles the inner regions of planetary magnetospheres, these laboratory observations are linked to space plasma physics. Unlike many other toroidal configurations, interchange and entropy modes dominate plasma dynamics, and turbulence causes self-organization and centrally-peaked profiles as the plasma approaches a state of minimum entropy production.

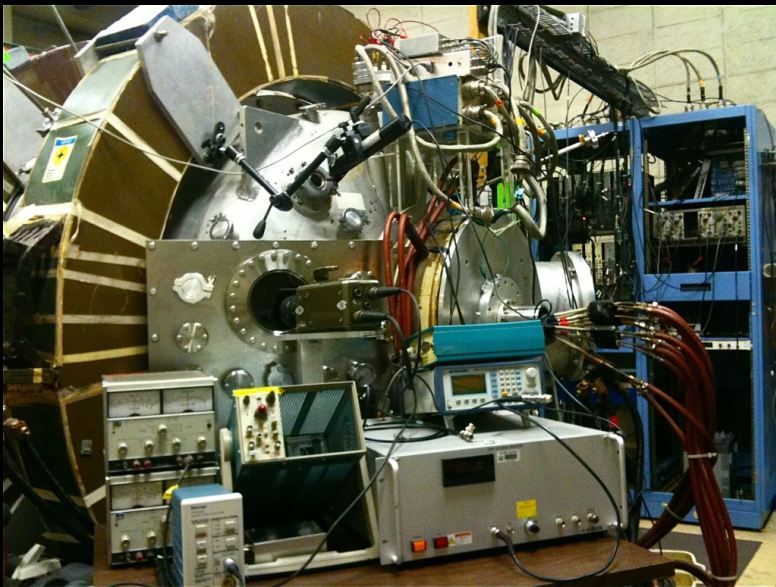
We report progress in understanding and controlling turbulent mixing through a combination of laboratory investigation, modeling, and simulation. Topics discussed:

- (i) Extending the global extent of local regulation of the interchange and entropy mode turbulence through current injection,
- (ii) Measurement and interpretation of the statistical properties of stationary turbulence, and
- (iii) Advancements in the nonlinear simulation of turbulence control in a dipole plasma torus.

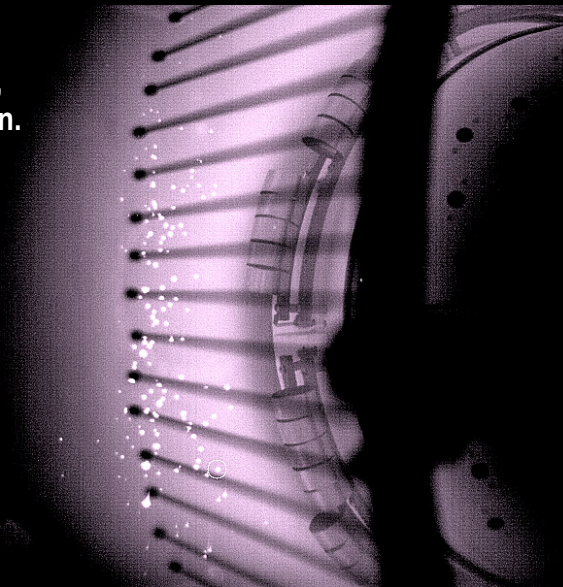
Two Laboratory Magnetospheres: Plasma Experiments without Field-Aligned Currents



LDX:
High Beta Levitation & Turbulent Pinch



CTX:
Polar Imaging,
Current Injection,
Rotation



Toroidal Confinement with Closed-Field Lines: Interchange and Entropy Modes

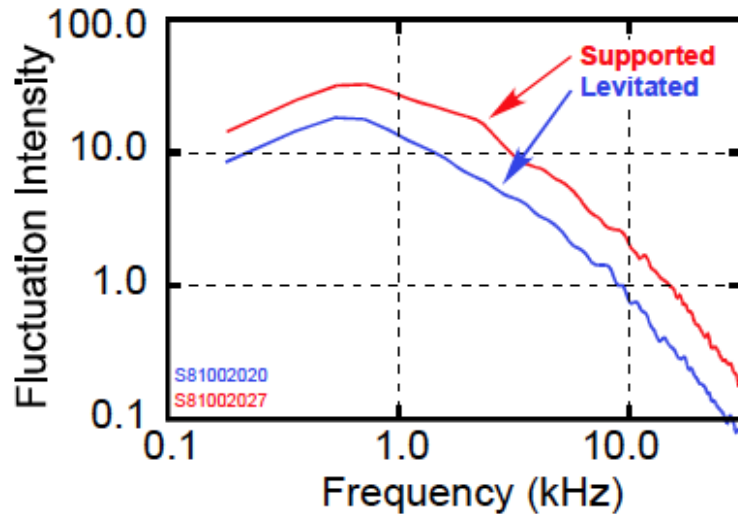
- Axisymmetric magnetically dipole *guarantees omnigeneous particle drifts*.
- The only high- β toroidal magnetic configuration that satisfies the Palumbo condition: *the divergence of the perpendicular plasma current vanishes*.
- Absence of parallel currents in a dipole-confined plasma is significant: *many tokamak instabilities are not found in a dipole plasma torus*, e.g. kink, tearing, ballooning, and drift modes.
- Instead, interchange and entropy modes dominate plasma dynamics, and *particle and power source profiles determine the level of turbulence*.
- Turbulent transport causes *centrally-peaked profiles and self-organization*, as the plasma approaches a *state of minimum entropy production*.
- Axisymmetric interchange/entropy mode *turbulence exhibit 2D inverse cascade at long wavelengths*.

Closed Field-Line Plasma Dynamics

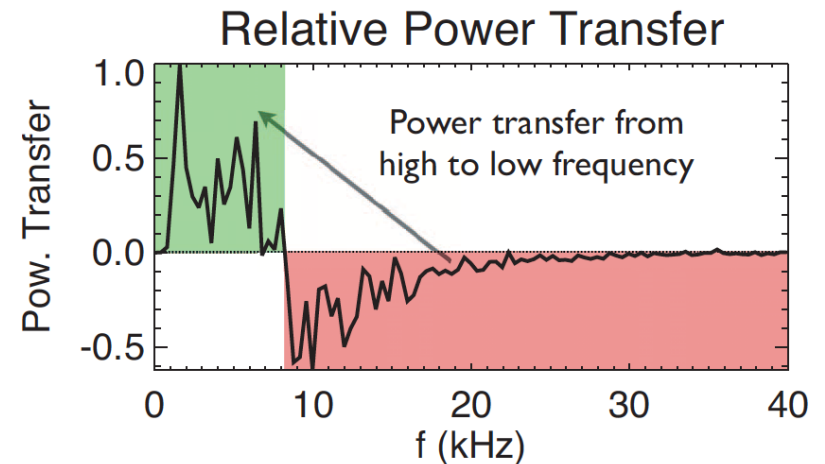
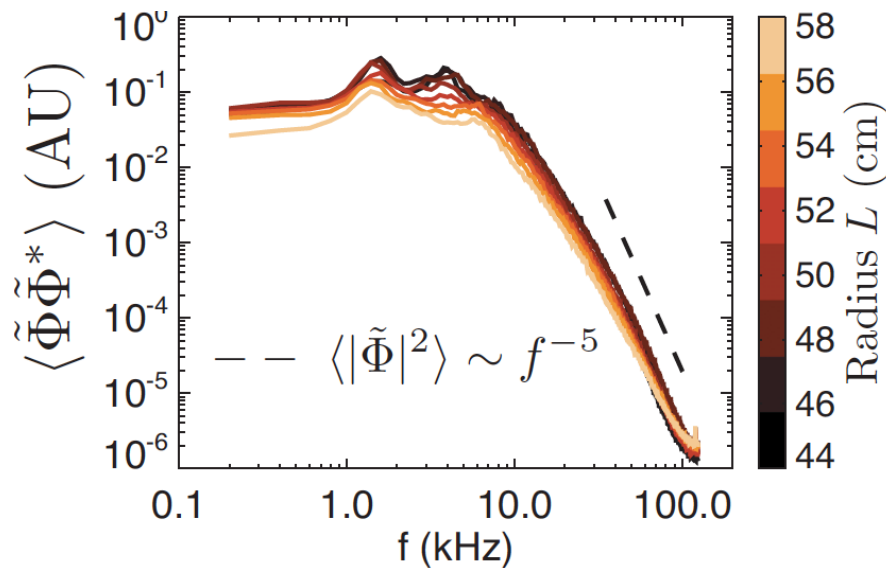
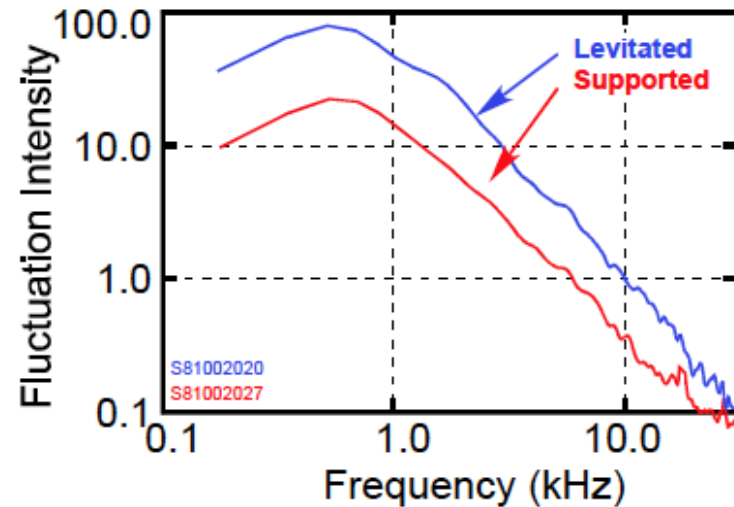
- How do we know dynamics is “interchange” dominated?
 - ➔ *Direct laboratory measurement of $\delta\Phi$, in **all cases**, but when $\omega_{be} \gg \omega_d$*
- What are the consequences of “interchange” dynamics?
 - ➔ *2D inverse cascade couples fluctuations to largest scales*
 - ➔ *“Weak gradients” with $\omega^* \sim \omega_d$*
 - ➔ *Profile consistency, turbulent pinch, ...*
 - ➔ *Self-organization toward state of minimum entropy production, $\eta \sim 2/3$*

Turbulent Intensity is Observed to Peak at Long Wavelengths (Inverse Mode-Mode Cascade)

(a) Edge Floating Potential Fluctuations

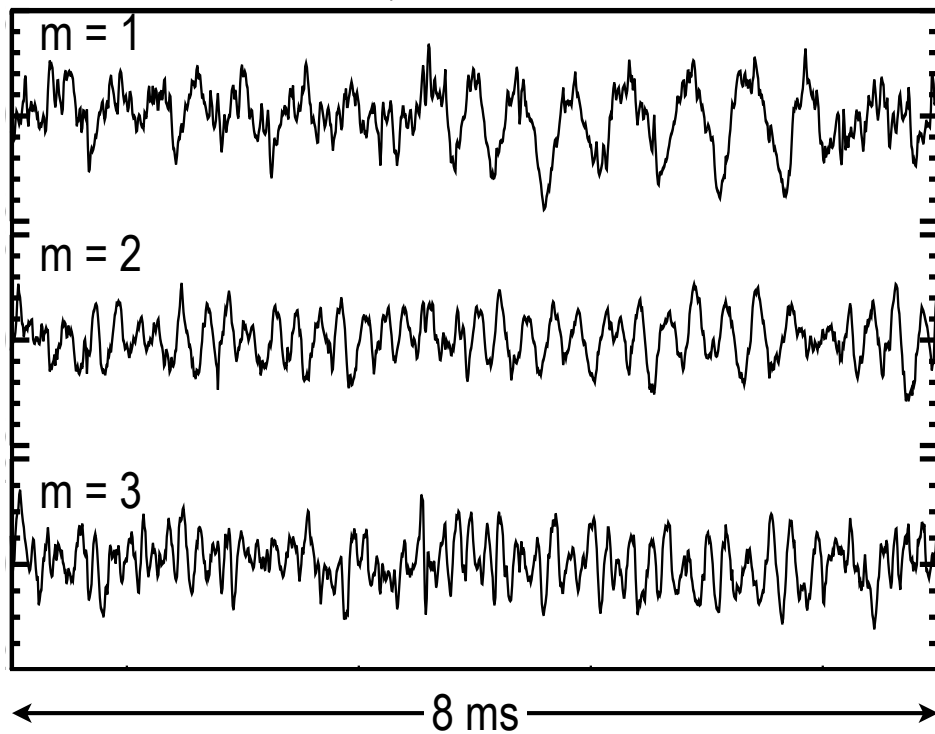
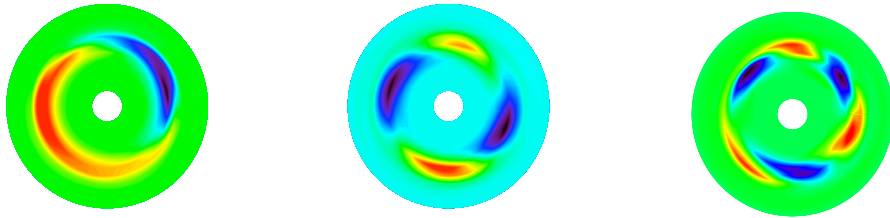


(b) Inner Interferometer Fluctuations

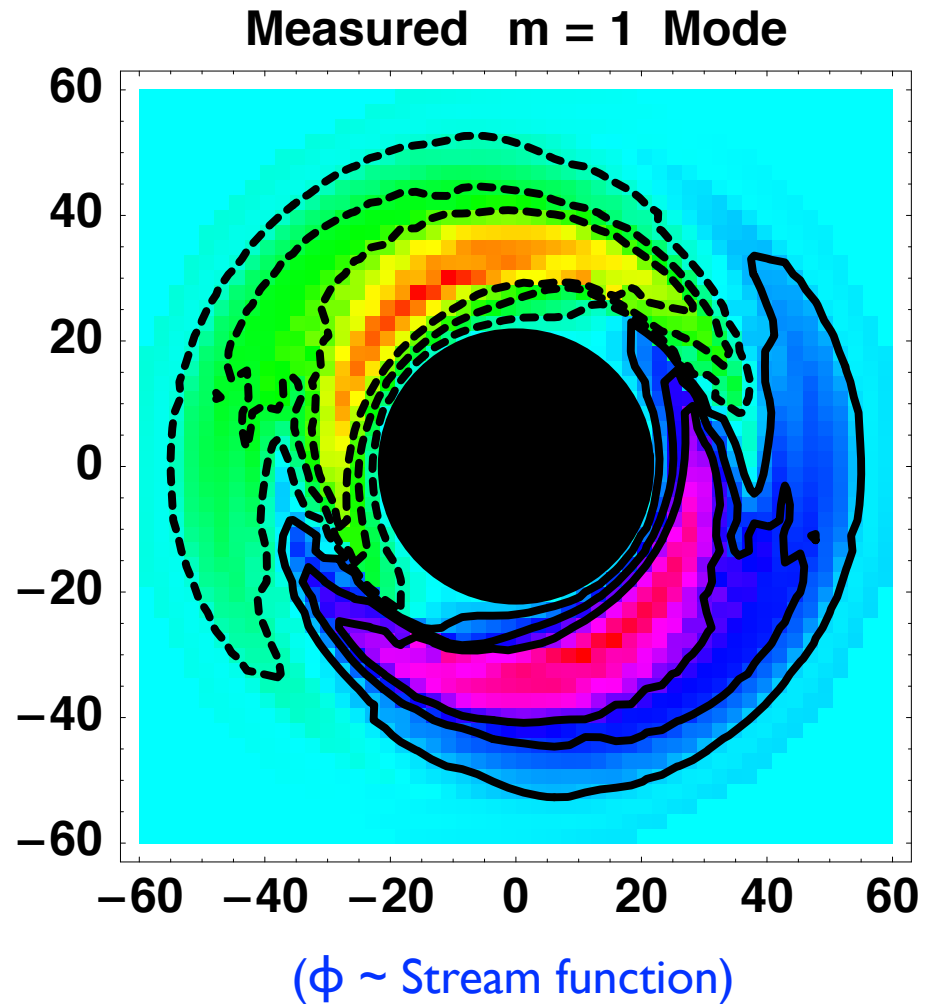


Grierson, M. Worstell, and M. Mauel, *Phys Plasmas* **16**, 055902 (2009).
 Boxer, et al., *Nature Phys* **6**, 207 (2010).

Measured Interchange Modes in Dipole Torus



Convective Structures are Dynamic



With $T_e \gg T_i$ (CTX and LDX) modes (usually) propagate in electron drift direction

Induced Field-Aligned Currents in Magnetospheres

$$U_{con} \cong \frac{c^2}{8\pi \Sigma_p} \cdot \frac{\ell_{\parallel}}{L_{ps}} \cdot \ell_n \left(\frac{p_{tot}^{(24)}}{p_{tot}^{(12)}} \right)$$

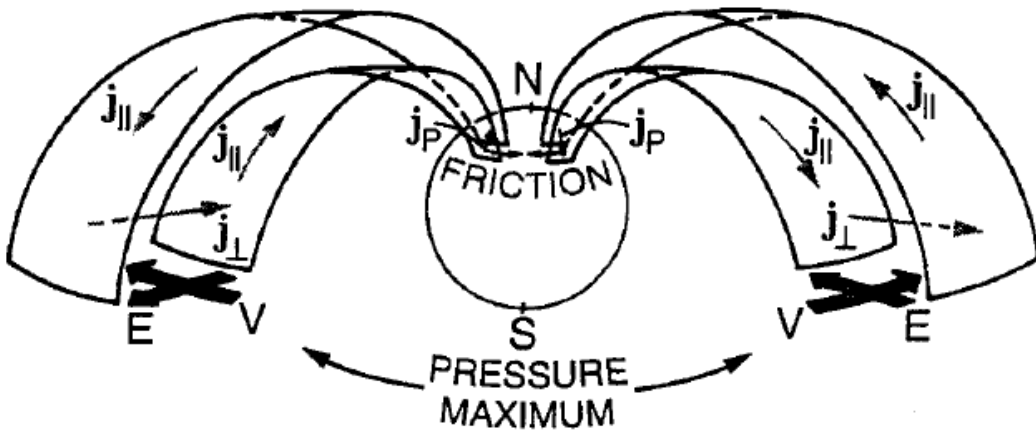


Figure 3. Dynamo forces, auroral current system, and resulting convection under frictional control by the ionosphere, after Boström (1964).

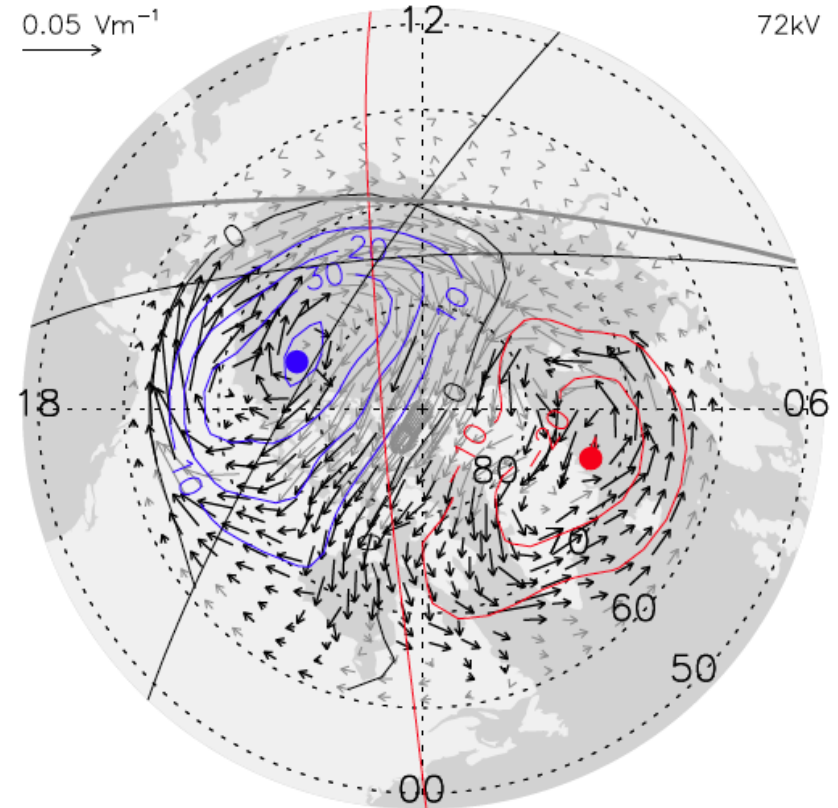
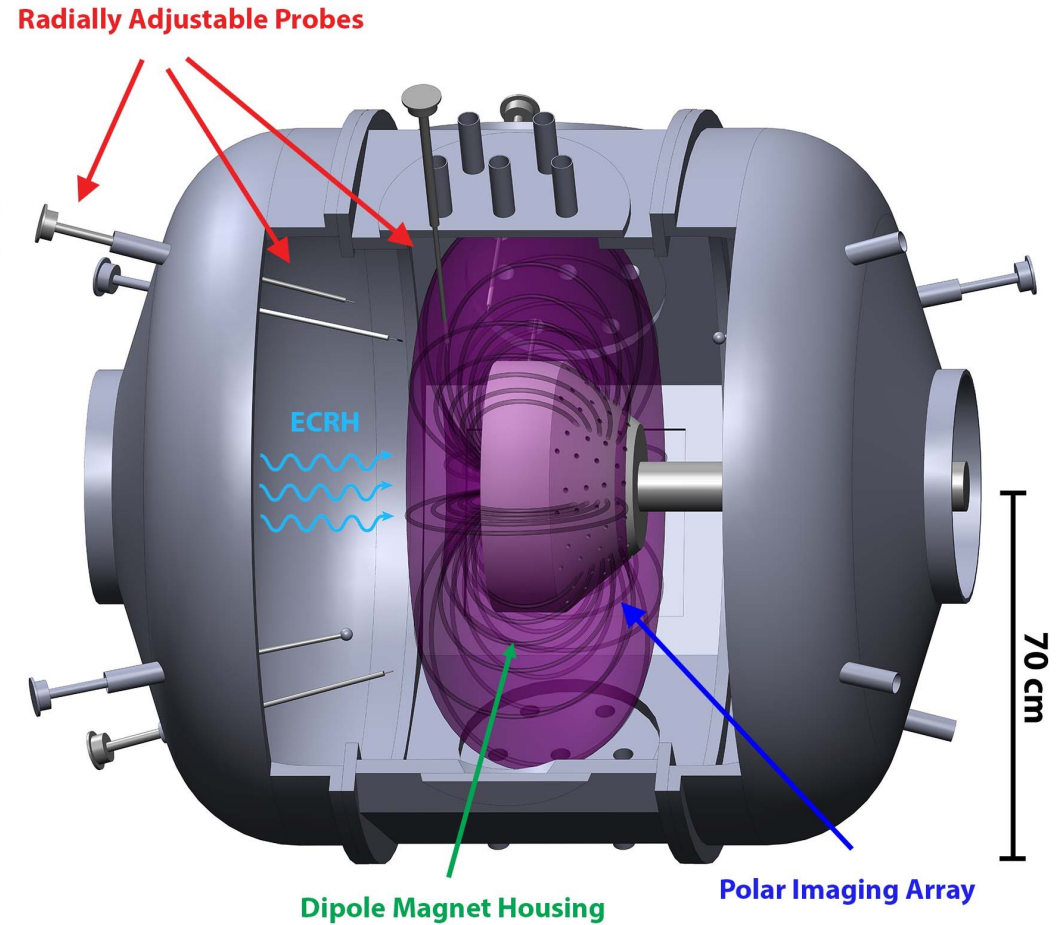
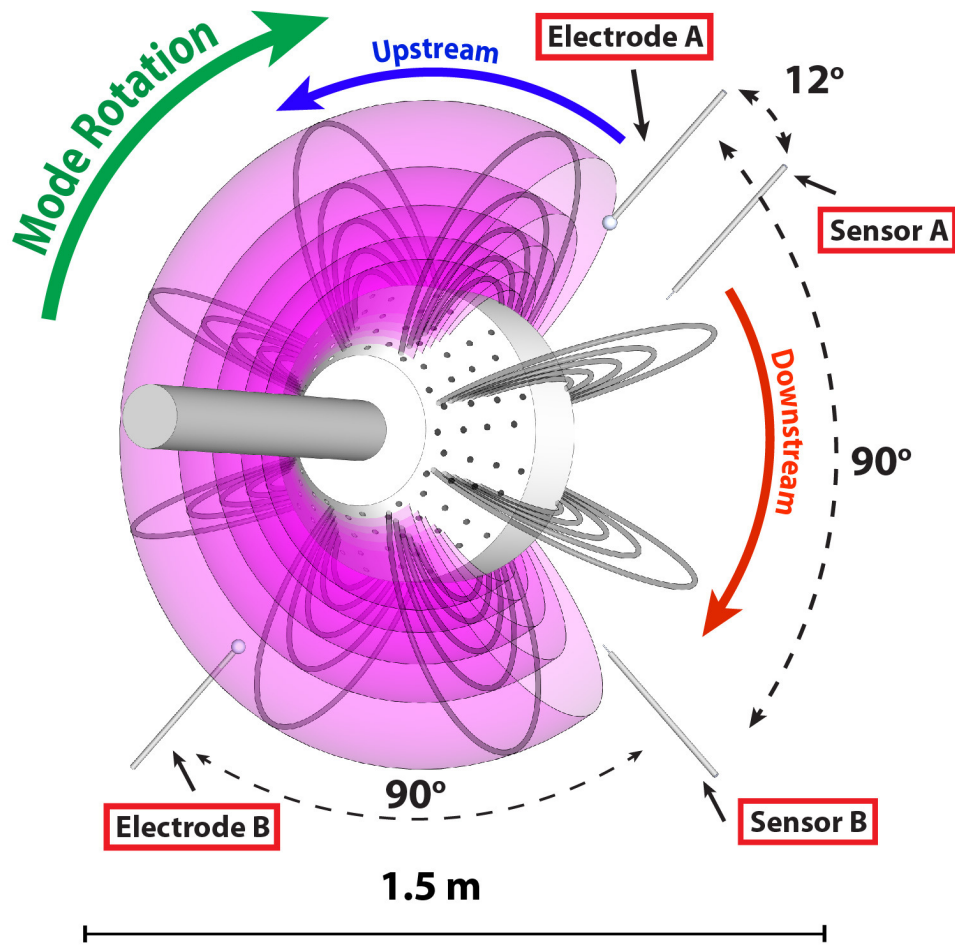


Fig. 7. Electric field vectors (rotated 90° counter clockwise) calculated from SuperDARN data averaged over 03:30–04:30 UT, 1 November, 2001. The electric potential contours, DMSP and Oersted tracks and the sunlight terminator are overlaid. The extremes in potential are located at the blue (-ve) and red (+ve) dots. The electric field vectors are bold at locations where radar returns were received.

G. Haerendel, "Outstanding issues in understanding the dynamics of the inner plasma sheet ...," *Advances in Space Research*, **25**, 2379 (2000).
 Green, et al., "Comparison of large-scale Birkeland currents determined from Iridium and SuperDARN data," *Annales Geophysicae* **24**, 941 (2006).

Probe-Injected Currents in Laboratory



Roberts, *et al.*, "Local regulation of interchange turbulence in a dipole-confined plasma torus using current-collection," *Physics of Plasmas*, **22**, 055702 (2015).

Interchange Motion is Regulated by Ionosphere, or External Circuits, or ...

$$\int \frac{ds}{B} \nabla_{\perp} \cdot \mathbf{J}_{\perp} = \begin{cases} 0 & \text{Closed, insulated, field lines} \\ 2(J_{\parallel}/B)_{poles} & \text{Ionospheric current} \\ \sum_j I_j \delta(\psi - \psi_j) \delta(\phi - \phi_j) & \text{External circuits} \end{cases}$$

Steady MHD Convection in Space

$$\hat{\mathbf{b}} \cdot \nabla \Phi = 0$$

Dynamic Drift-like Motion in Lab

$$\mathbf{J}_{\perp} = \frac{\hat{\mathbf{b}} \times \nabla P}{B} \quad (\text{space})$$

$$\frac{2J_{\parallel}}{B_{pole}} = \nabla_{\perp} P \cdot \hat{\mathbf{b}} \times \nabla_{\perp} \int \frac{ds}{B}$$

$$\nabla_{\perp} \cdot \Sigma_p \nabla_{\perp} \Phi \approx -J_{\parallel} (\hat{\mathbf{b}} \cdot \hat{\mathbf{n}}) \quad (\text{poles})$$

Ionospheric Conductivity

$$\mathbf{J}_{\perp} = \frac{\hat{\mathbf{b}} \times \nabla P}{B} - \frac{nM_i}{B^2} \nabla_{\perp} \frac{d\Phi}{dt}$$

Ion Inertial Currents

$$\int \frac{ds}{B} \nabla_{\perp} \cdot \mathbf{J}_{\perp} = 0$$

$$\nabla_{\perp} \cdot \bar{\Sigma} \cdot \nabla_{\perp} \frac{\partial \Phi}{\partial t} \approx -\nabla_{\perp} P \cdot \hat{\mathbf{b}} \times \nabla_{\perp} \int \frac{ds}{B}$$

Integrated Plasma Dielectric

Vasyliunas, "Mathematical Models of Magnetospheric Convection and Its Coupling to the Ionosphere," in *Particles and Fields in the Magnetosphere*, edited by B.M. McCormac (D. Reidel, Norwell, MA, 1970), pp. 60–71.

Entropy & Drift-Interchange Modes

(For CTX and LDX with $T_e \gg T_i$)

ω_{de} flow

Collisionless heat flux due to
Electron magnetic drift

$$\frac{\partial \tilde{N}}{\partial t} + \frac{dh_n}{dy} \frac{\partial \tilde{\Phi}}{\partial \varphi} + \frac{4}{y^5} \frac{\partial \tilde{P}_e}{\partial \varphi} = 0$$

$$\frac{\partial \tilde{P}_e}{\partial t} + y^{4\gamma} \frac{dh_g}{dy} \frac{\partial \tilde{\Phi}}{\partial \varphi} + \gamma \frac{4}{y^5} \left(\frac{y^{4\gamma} h_g}{h_n} \right) \left[2 \frac{\partial \tilde{P}_e}{\partial \varphi} - \left(\frac{y^{4\gamma} h_g}{h_n} \right) \frac{\partial \tilde{N}}{\partial \varphi} \right] = 0$$

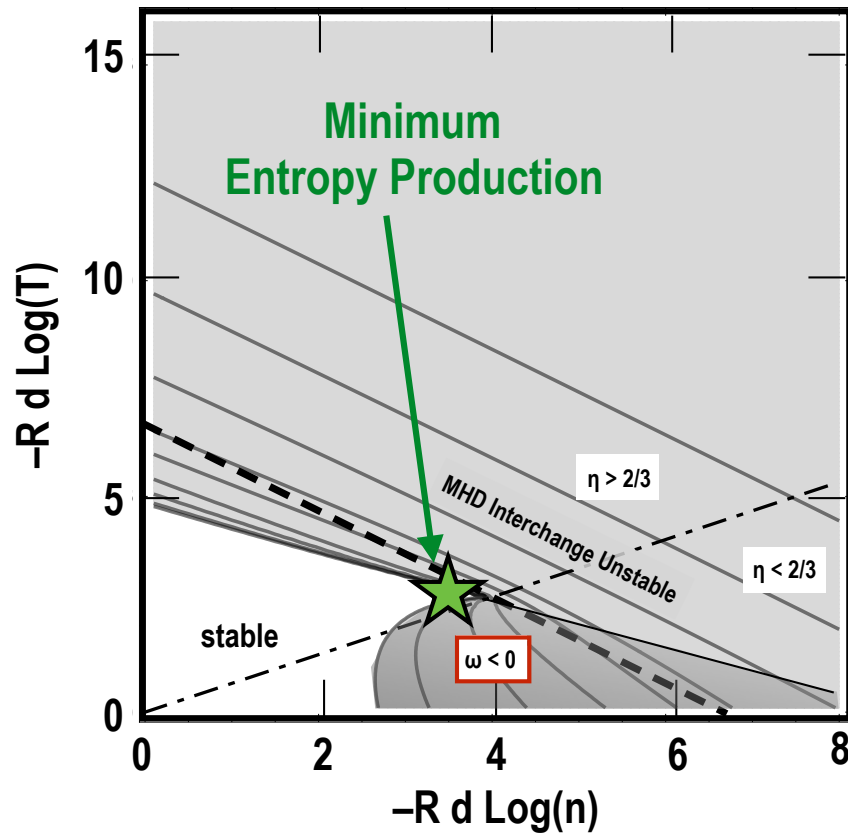
$$\rho_*^2 \left(\frac{\partial}{\partial t} + \nu_i \right) \left[\frac{\partial}{\partial y} \left(h_n \Sigma_\psi \frac{\partial \tilde{\Phi}}{\partial y} \right) + h_n \Sigma_\varphi \frac{\partial^2 \tilde{\Phi}}{\partial \varphi^2} \right] + \frac{4}{y^5} \frac{\partial \tilde{P}_e}{\partial \varphi} = 0$$

ion-neutral
damping

Linear Braginskii interchange motion

Gradient Drive for Turbulent Transport: Comparing to the Familiar Tokamak...

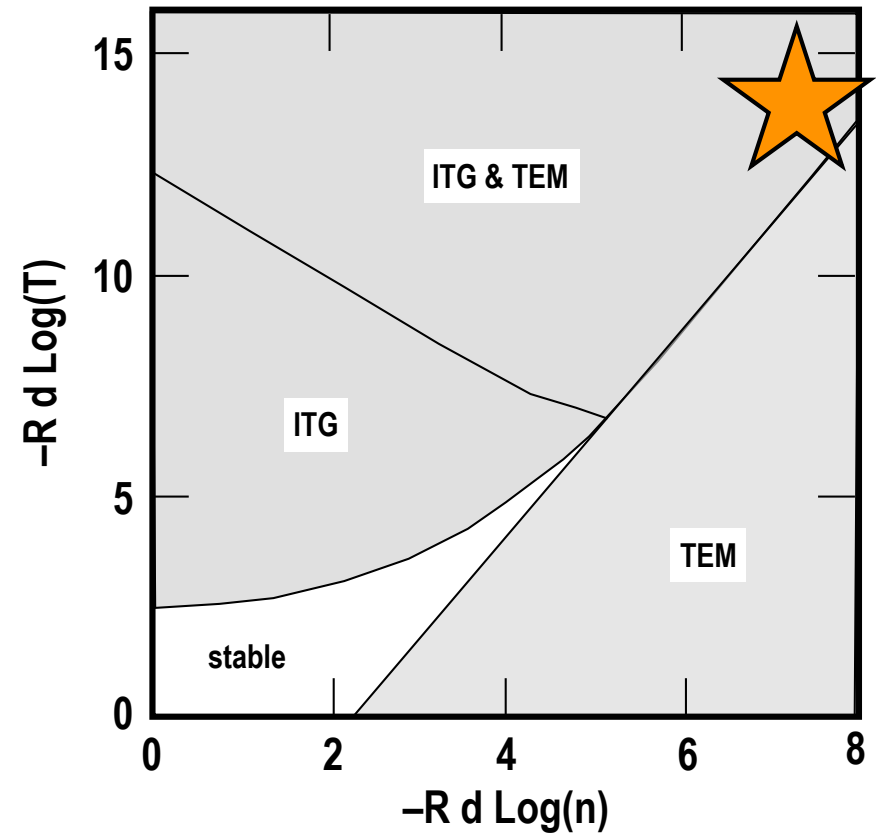
(a) Dipole Interchange-Entropy Modes



Weak gradients: $\omega_p^* \sim \omega_d$

Stable by compressibility and field line tension

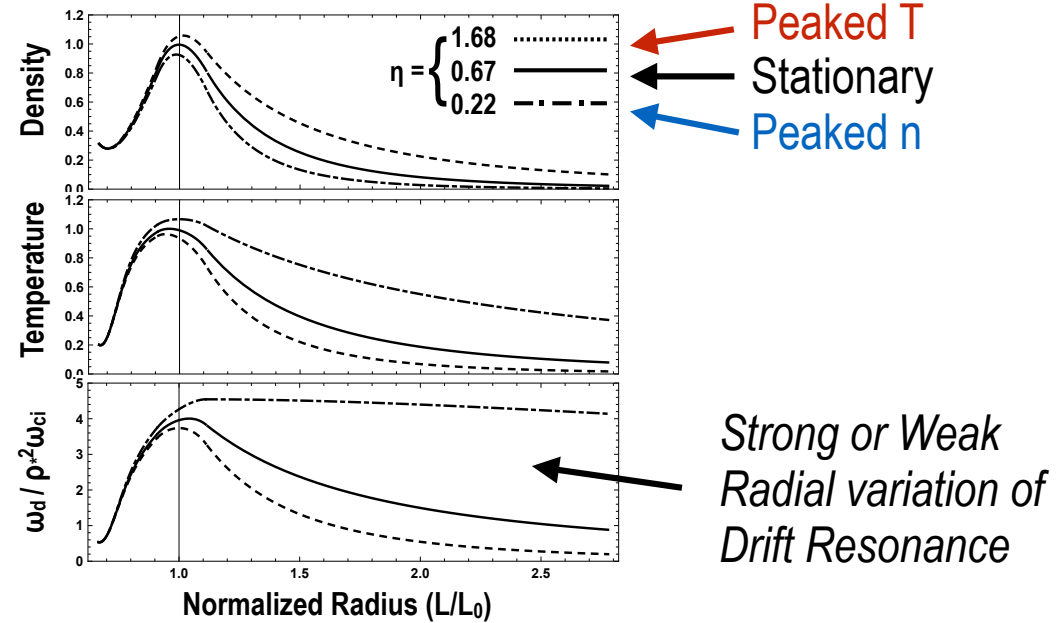
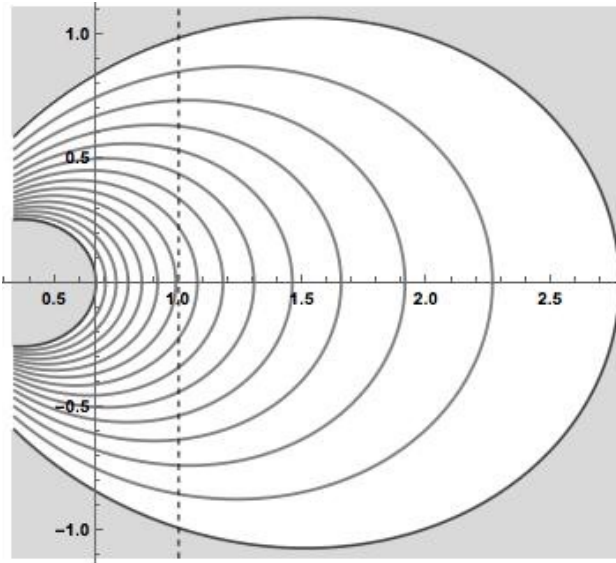
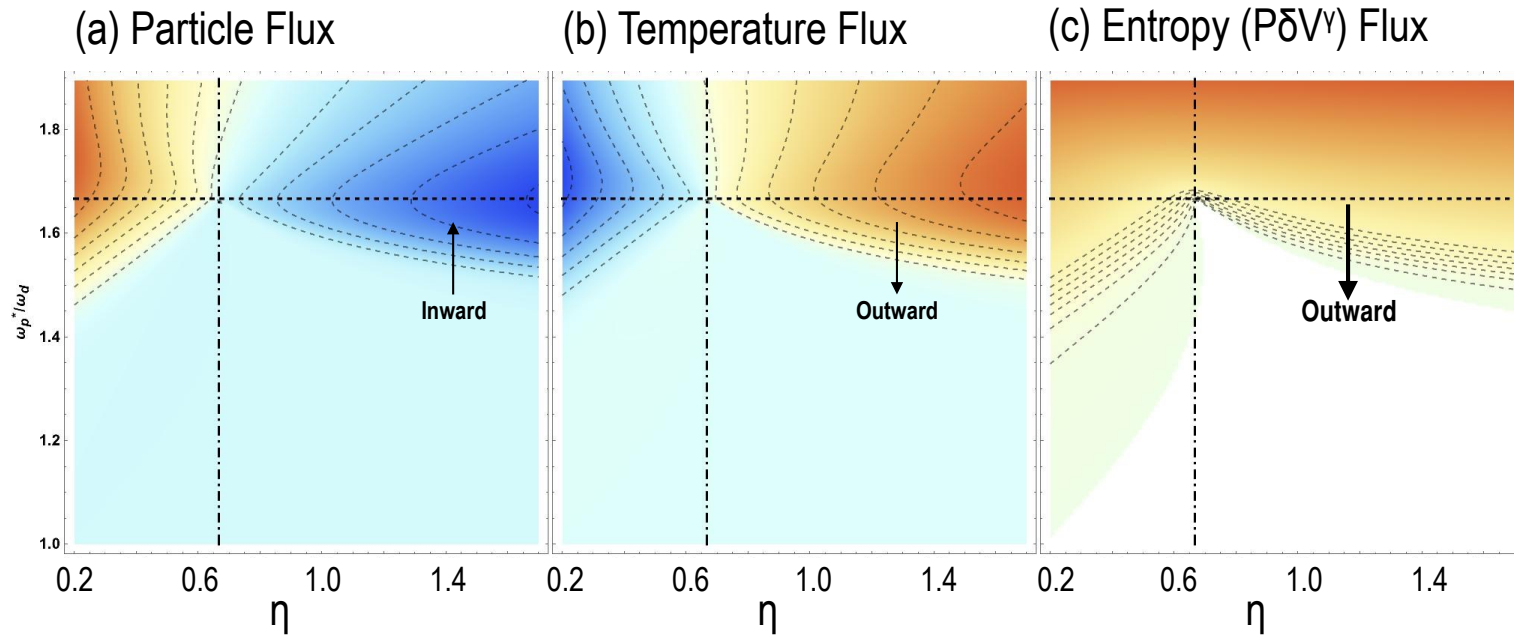
(b) Tokamak ITG-TEM Modes



Steep gradients: $\omega_p^* \gg \omega_d$

Stable by average curvature and magnetic shear

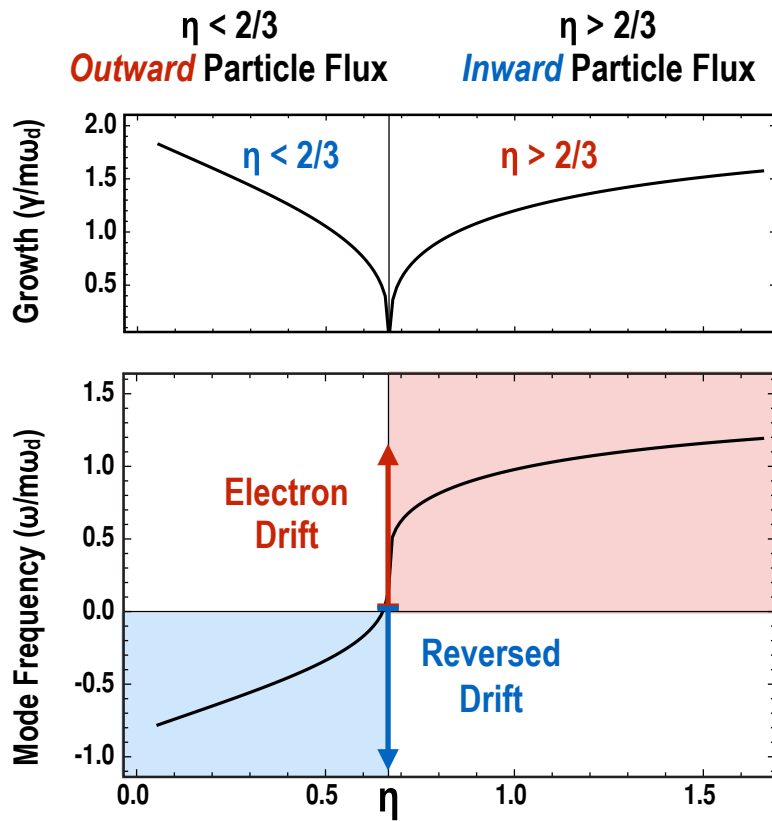
Quasilinear Flux using **2D** Bounce-Averaged Fluid Equations with Drift-Kinetic Closure



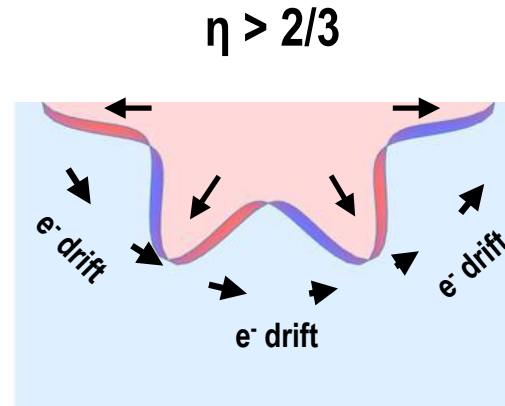
Kobayashi, Rogers, and Dorland, *Phys Rev Lett* **105**, 235004 (2010)

Interchange-Entropy Mode Dispersion Agrees with Observations

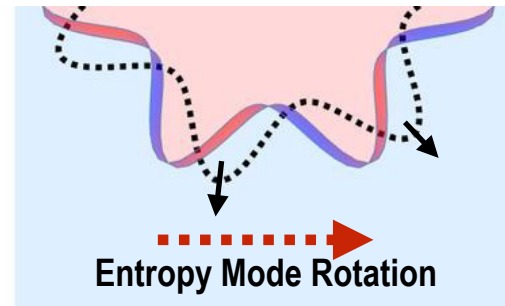
(a) Entropy Mode Dispersion: $\Delta W_p \sim \Delta(PV^{5/3}) \sim 0$



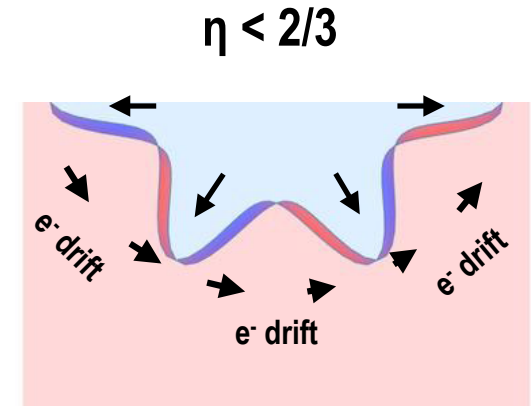
(b) “Warm Core” with Electron Drift



Drift-Kinetic **Heat** moves toroidally from **Warm** to **Cool** Flux-Tubes



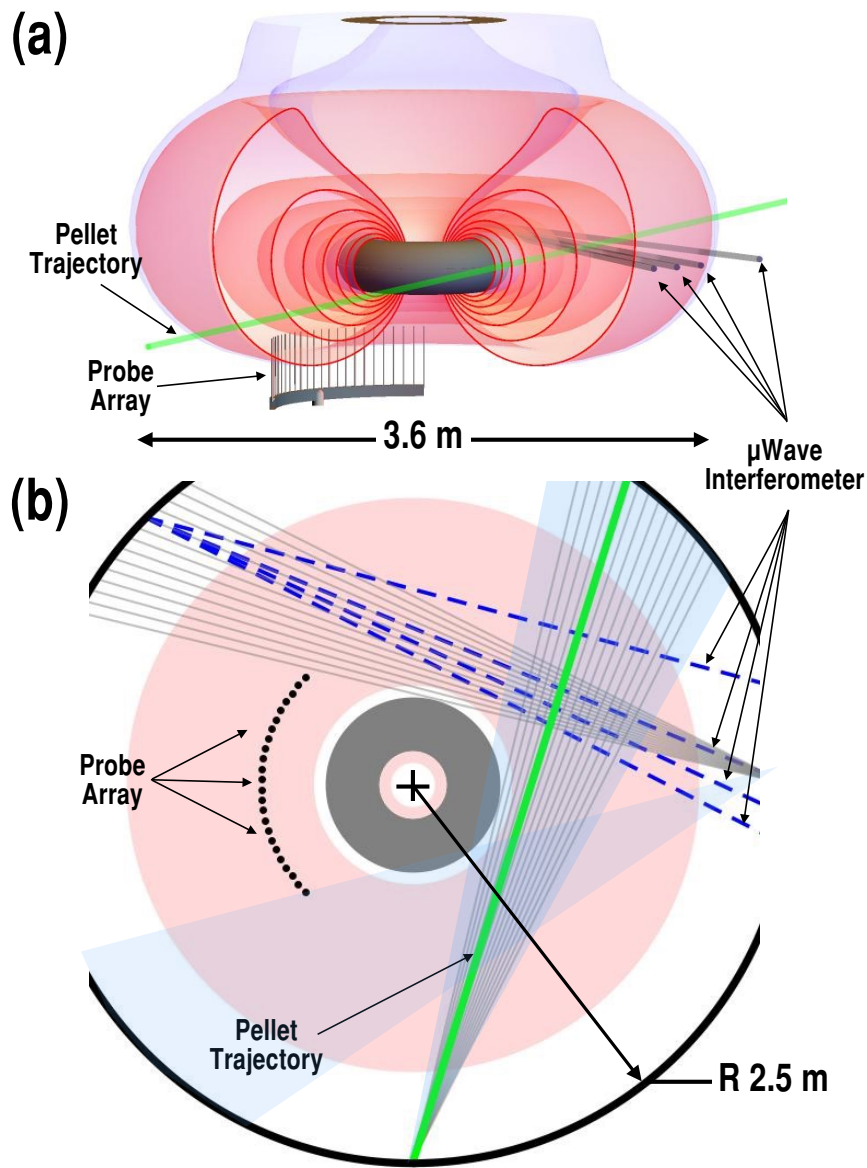
(c) “Cool Core” Reversed Rotation



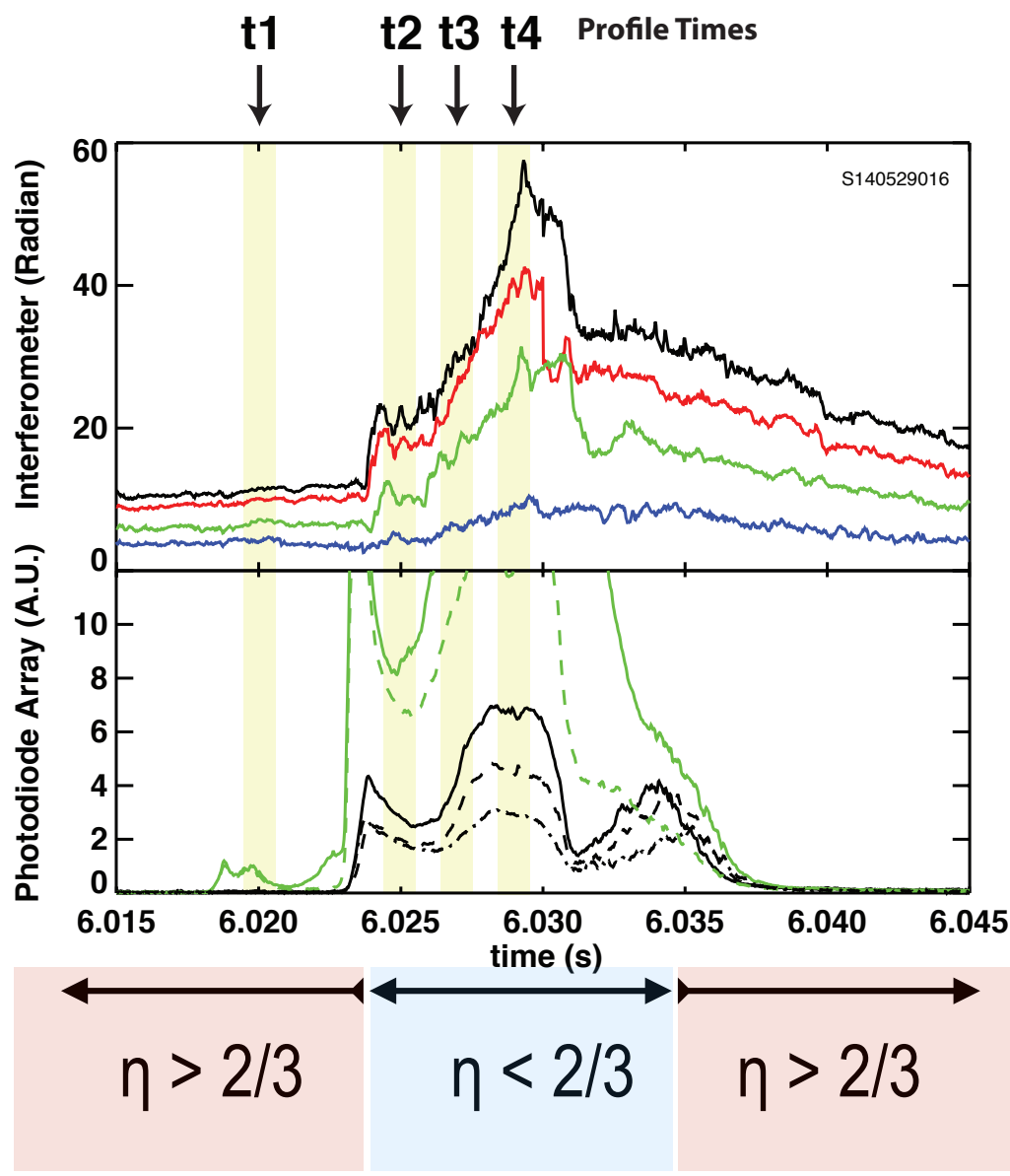
Entropy Mode Rotation

$$\frac{\partial \tilde{p}_e}{\partial t} + \underbrace{\frac{1}{\delta V^\gamma} \frac{\partial}{\partial \psi} (p \delta V^\gamma)}_{\text{Compressibility}} \frac{\partial \tilde{\Phi}}{\partial \varphi} - \underbrace{2\gamma \langle \kappa_\psi \rangle (T_e/e)}_{\text{Curvature Heat Flux}} \left[2 \frac{\partial \tilde{p}_e}{\partial \varphi} - T_e \frac{\partial \tilde{n}}{\partial \varphi} \right] \approx 0, \quad \omega \approx \frac{1}{(\rho_s^* m_\perp)^{2/3}} \begin{cases} \exp(i2\pi/3) (|\eta - 2/3|)^{1/3} & \text{if } \eta < 2/3 \\ \exp(i\pi/3) (\eta - 2/3)^{1/3} & \text{if } \eta > 2/3 \end{cases}$$

Entropy Modes Reverse with η (Pellet Injection)

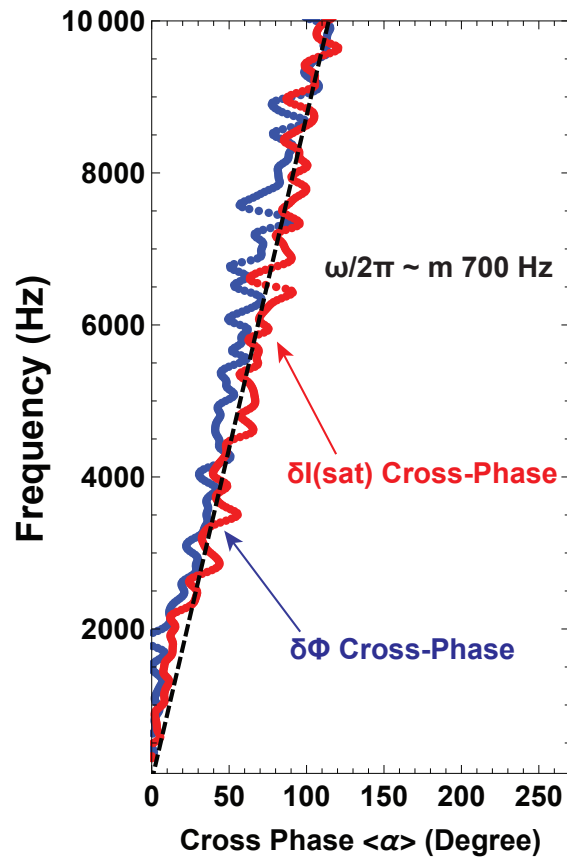


(a) Line Density and Photodiode Array



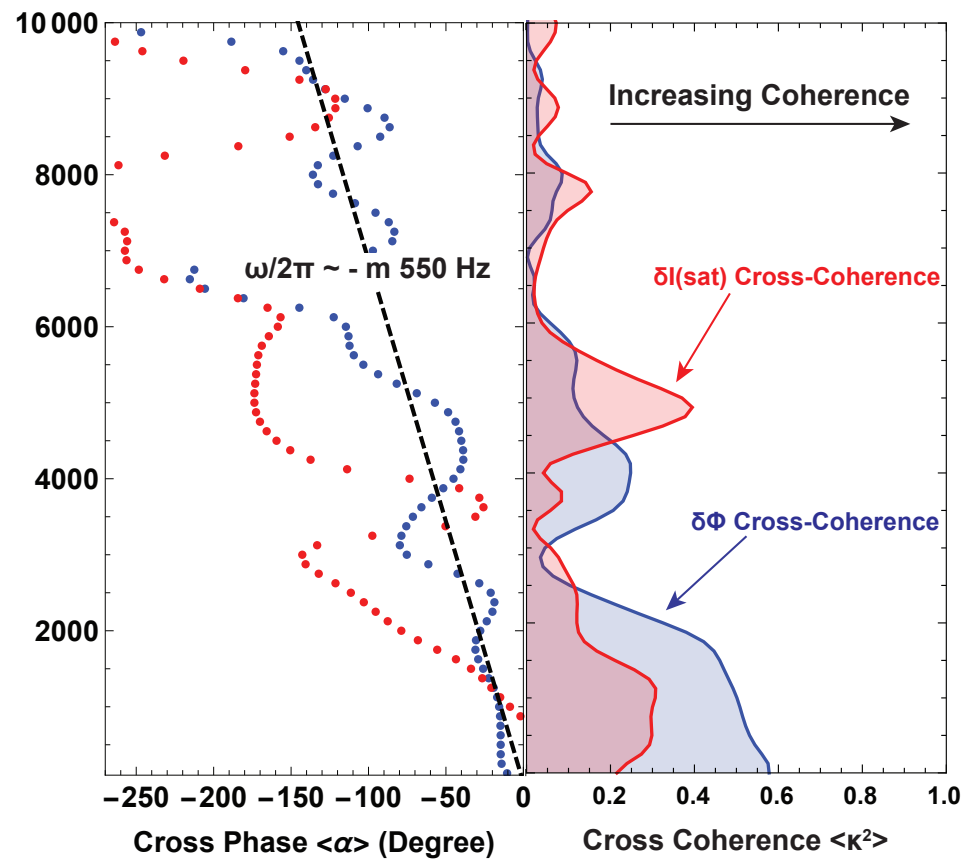
Entropy Modes Reverse with Pellet Injection

(a) Cross Phase Before Pellet



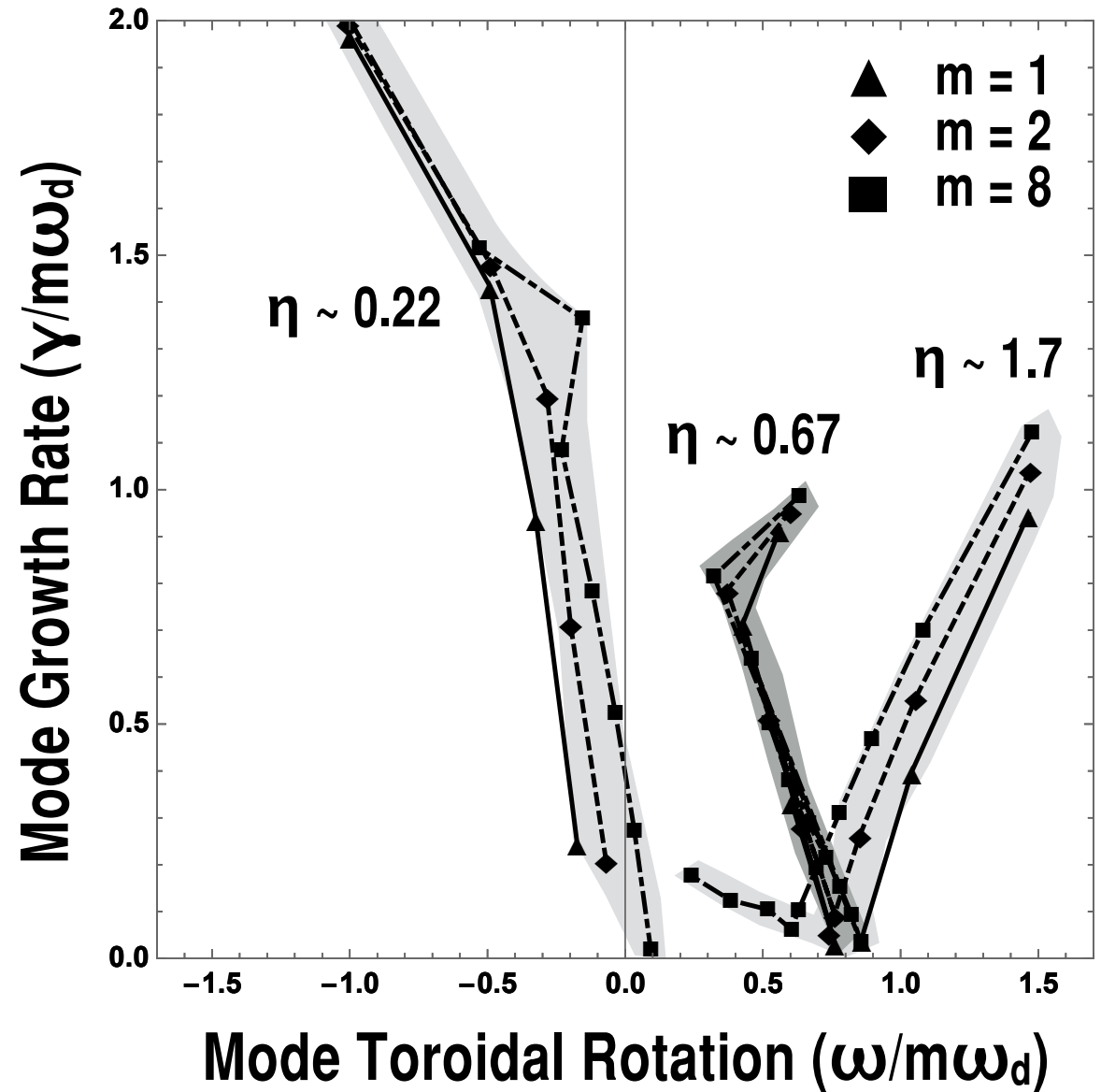
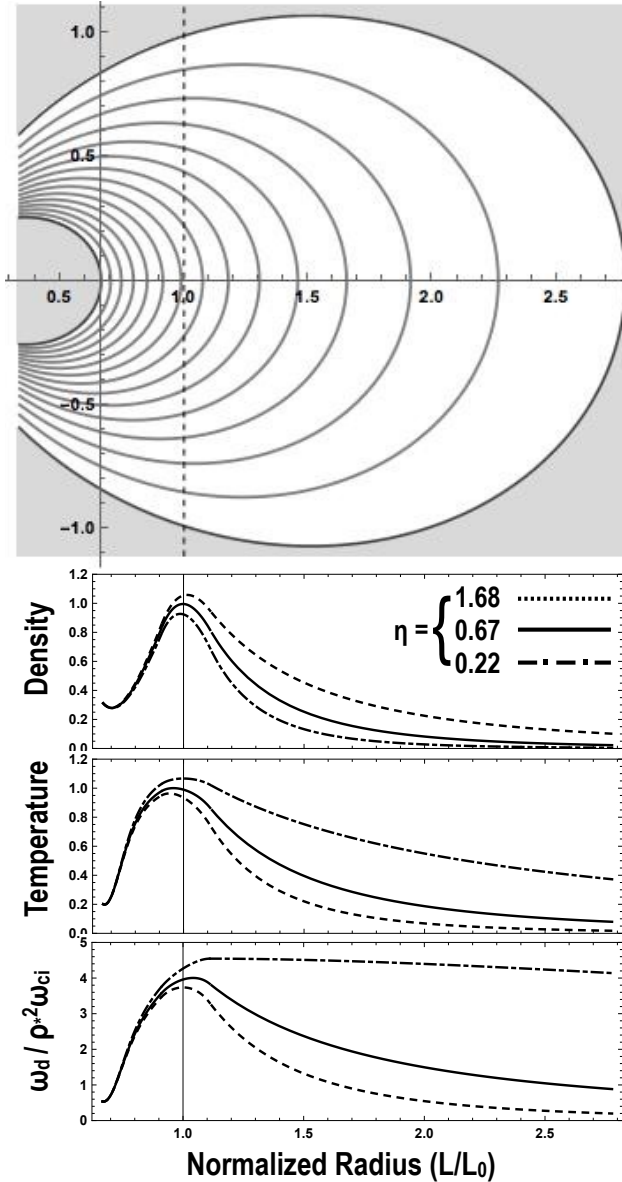
$\eta > 2/3$

(b) Cross Phase and Cross Coherence During Pellet



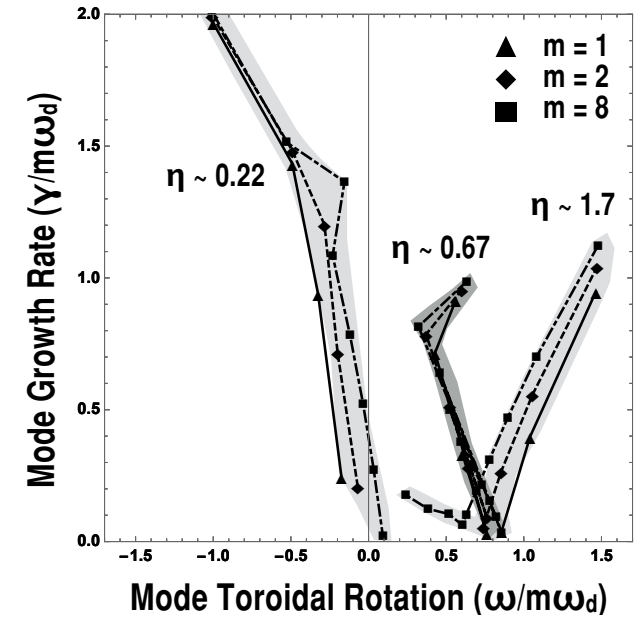
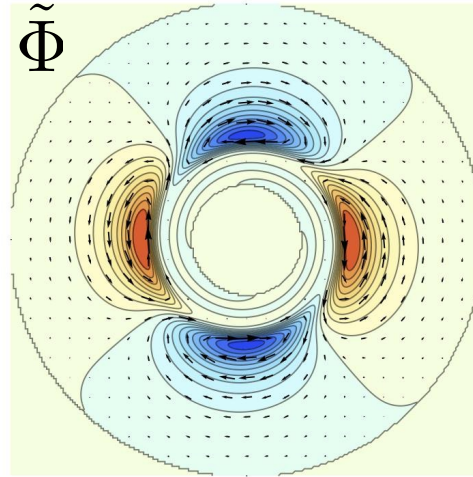
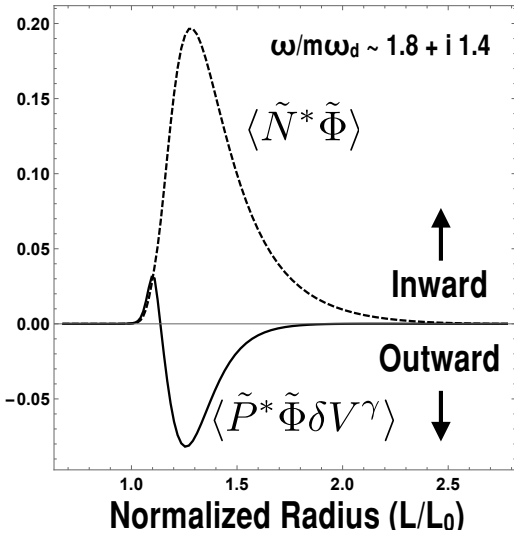
$\eta < 2/3$

Global Entropy Eigenmodes

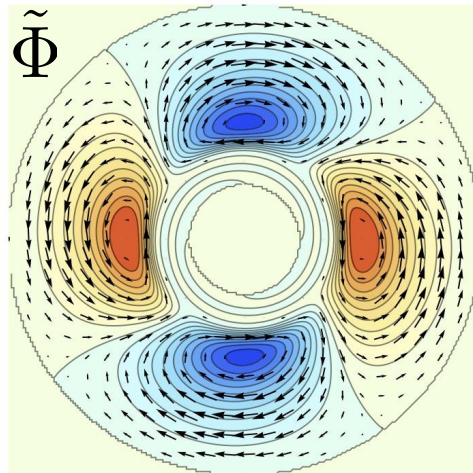
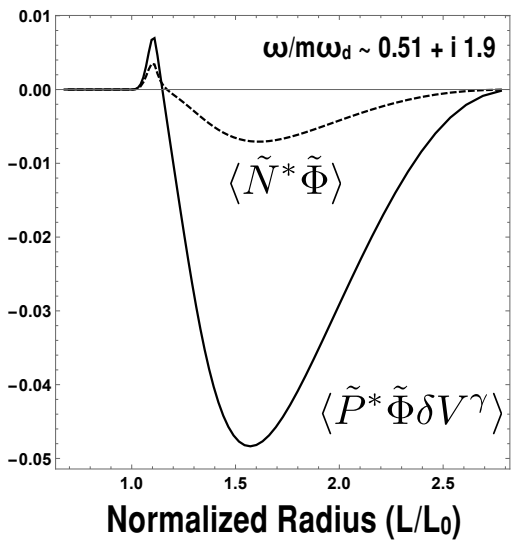


Global Entropy Eigenmodes

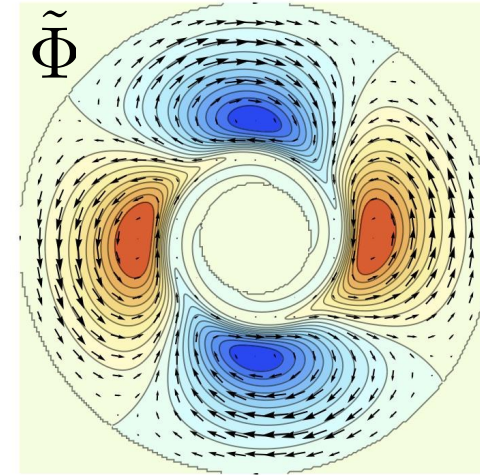
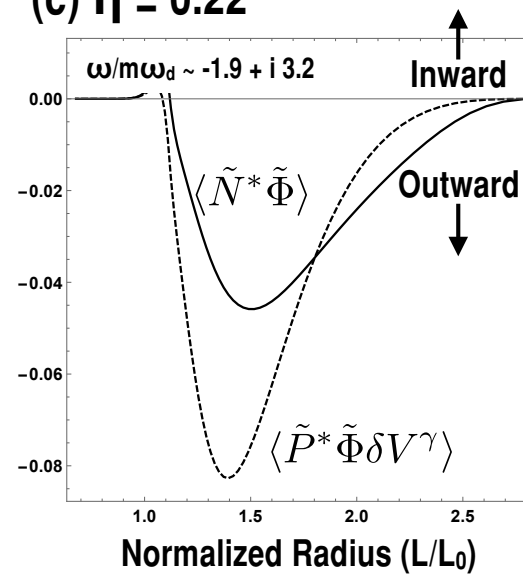
(a) $\eta = 1.68$



(b) $\eta = 0.67$



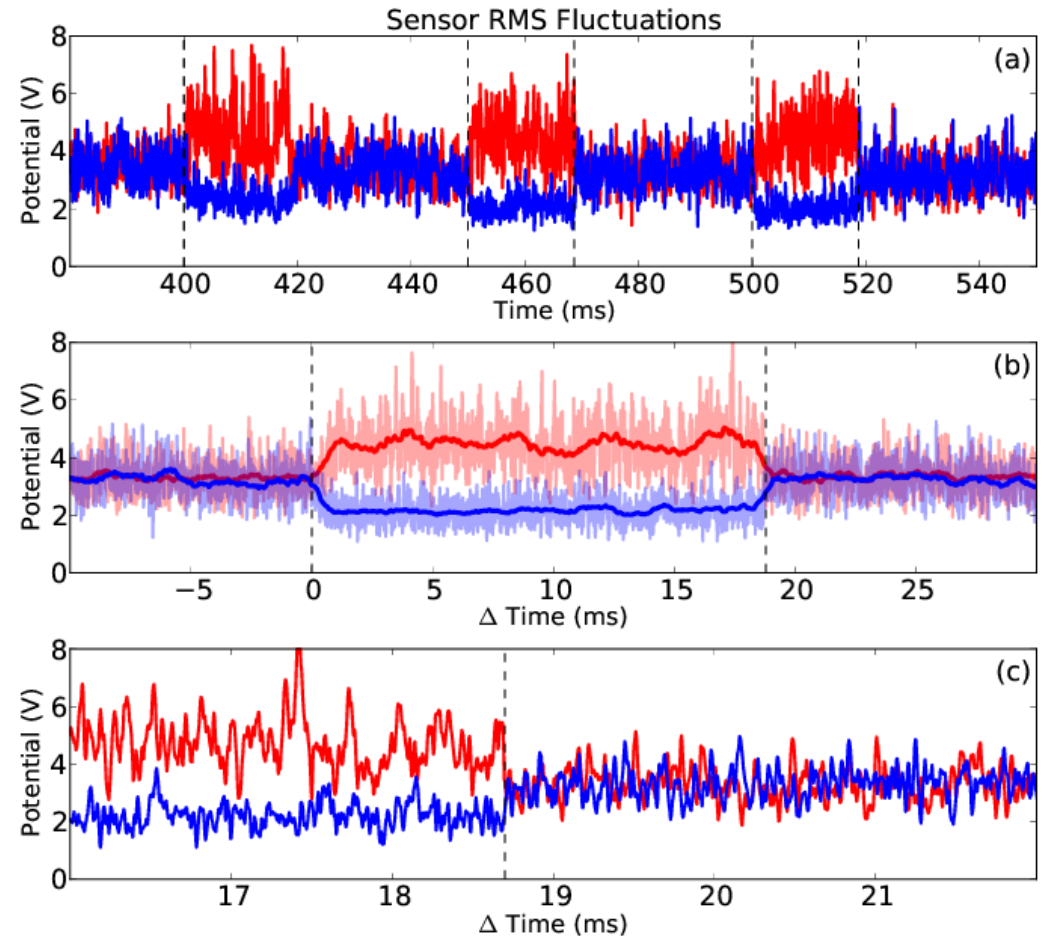
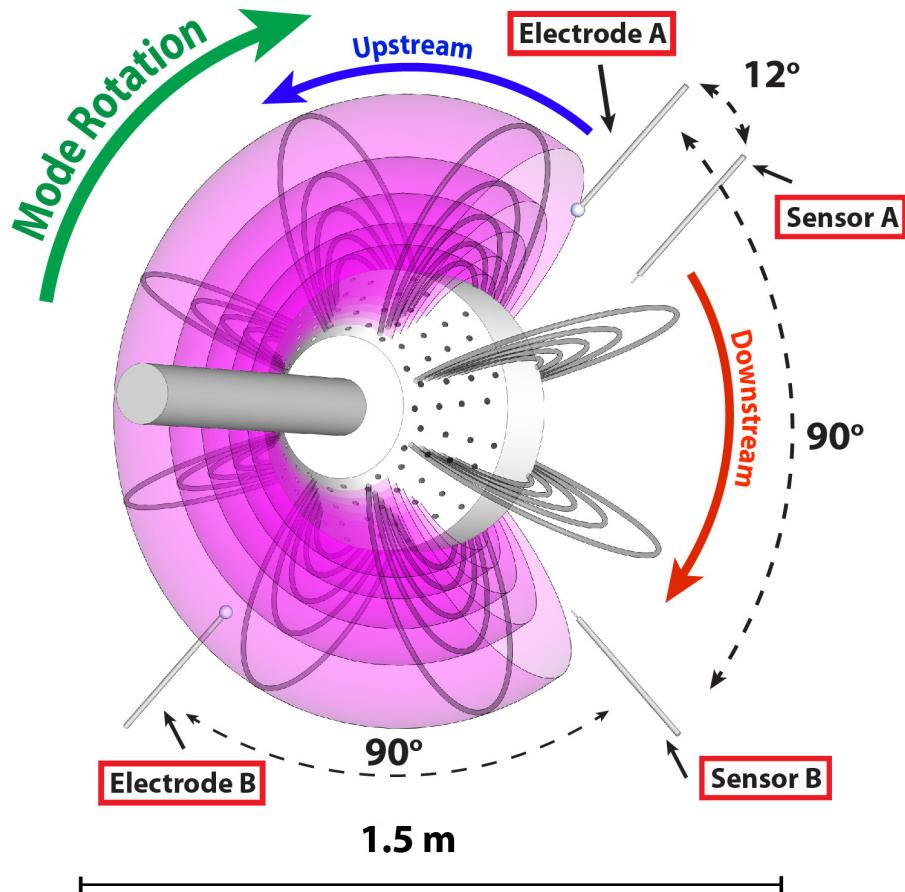
(c) $\eta = 0.22$



Summary and Applications

- Global flux-tube averaged gyro-fluid description of flute-type instabilities describes drift-interchange and entropy modes
- Long wavelength eigenmodes and real frequencies like observations in CTX and LDX
 - Quasilinear theory describes up-gradient turbulent pinches
 - Linear theory can model local current-injection feedback (Roberts, *PoP* 2015)
 - Li pellet injection reduces $\eta \rightarrow 0$ and reverses toroidal propagation of fluctuations
- Need to include bounce-averaged drift-resonances, like Maslovsky, Levitt, and Mael, *Phys Rev Lett* **90**, 185001 (2003) Beer and Hammett, *Phys Plasmas* **3**, 4018 (1996)
- Mode-mode and 2D interchange cascade may explain the discrepancy between observations dominated with low- m eigenmodes and linear high- m eigenmodes with large growth rates.
- Flux-tube averaging makes possible “whole-plasma” nonlinear turbulence simulations.

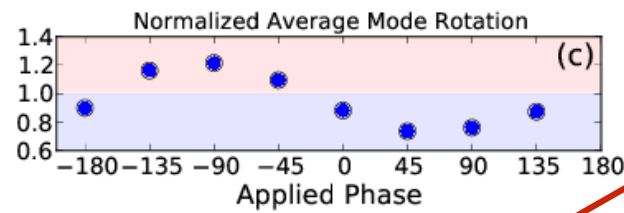
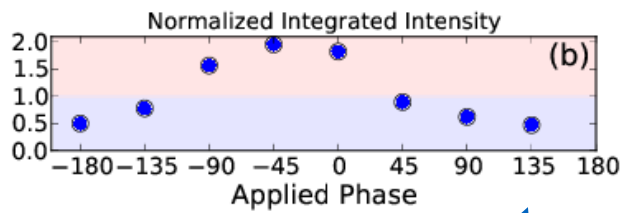
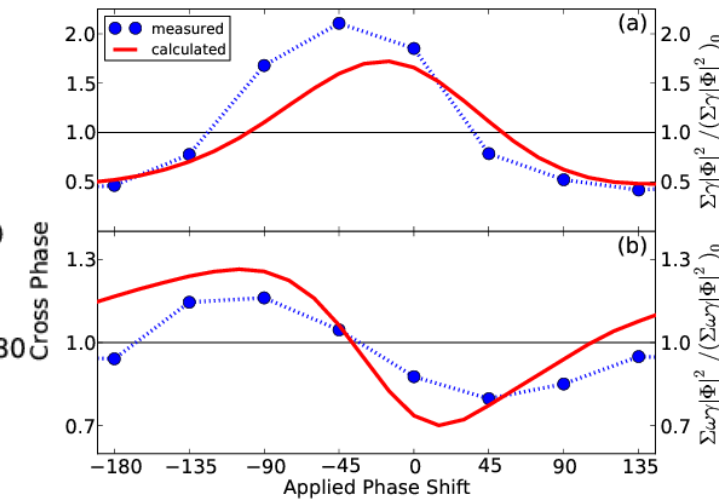
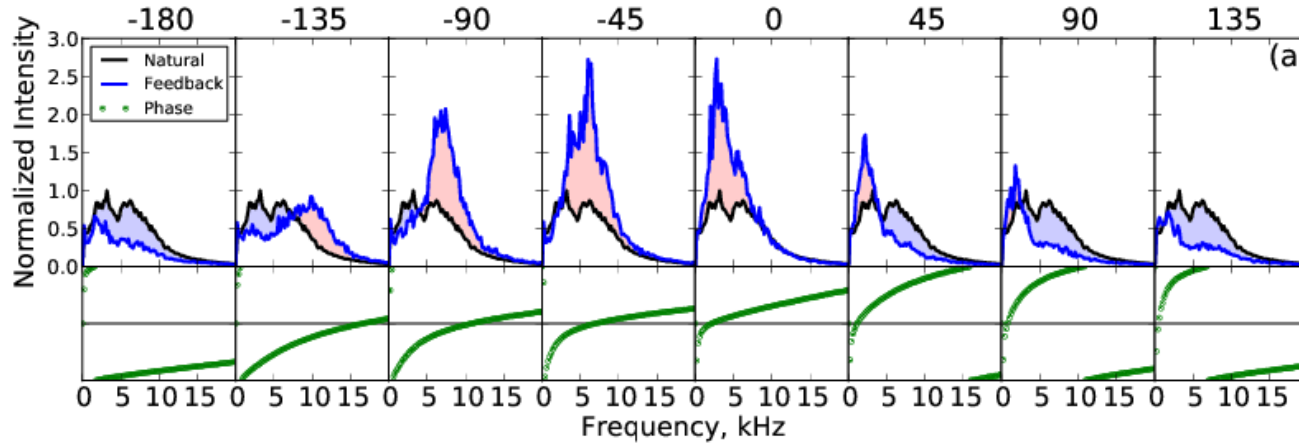
Single-Point Regulation of Interchange Turbulence with Current-Collection Feedback



Roberts, *et al.*, "Local regulation of interchange turbulence in a dipole-confined plasma torus using current-collection," *Physics of Plasmas*, **22**, 055702 (2015).

Local Regulation of Interchange Turbulence with Current-Collection Feedback

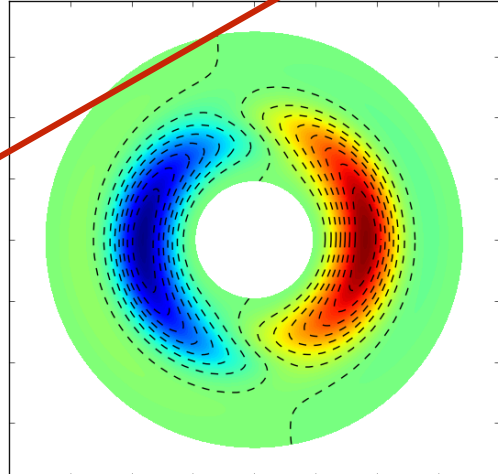
(Roberts, *Phys. Plasmas*, 2015)



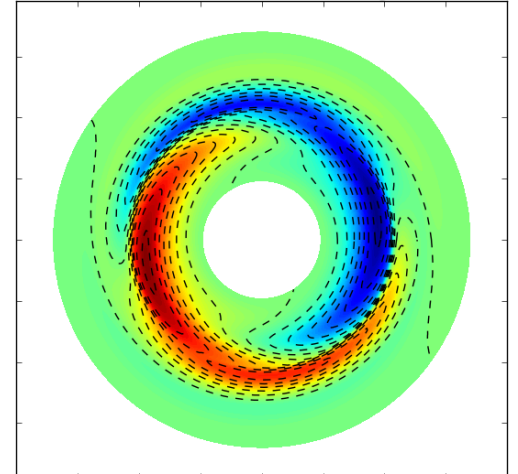
Measurement

Linear Theory

Electrostatic Potential Fluctuations



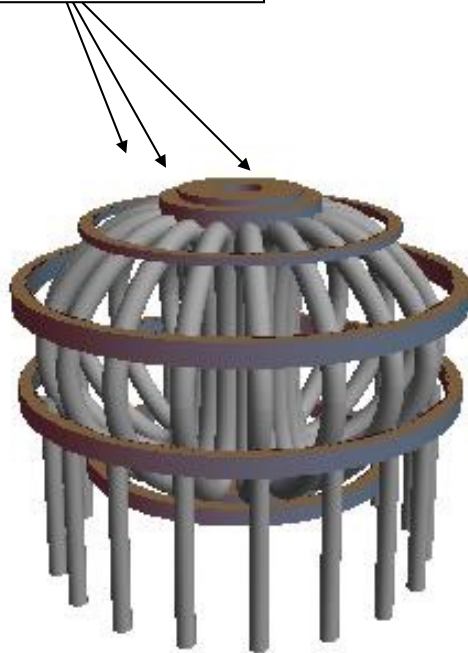
Perturbed Density



Application: Toroidal Confinement without B_t may Speed Fusion Development using *much smaller* Superconducting Coils ($Q_{DT} \sim 10$ Magnet Systems Compared at Same Scale)

Kesner, et al., *Nuclear Fusion* 44, 193 (2004)

Toroidal and Poloidal Magnets



Plasma Volume = 837 m³

$P_{fus} = 410$ MW $W_p = 1.1$ GJ $W_b = 51$ GJ $I_t = 164$ MA

(a) Conventional Fusion Experiment (Gain = 10)

Small Levitated Magnet



Plasma Volume = 42,000 m³

$P_{fus} = 39$ MW $W_p = 0.06$ GJ $W_b = 1.6$ GJ $I_d = 25$ MA

(b) Dipole Fusion Experiment (Gain = 10)

30-fold size/energy reduction (!)